fibers

MDPI

Article

Multilayer Electrospun Nanofibrous Membranes for Enhanced Heavy Metal Remediation

Magaly Granda [1], Ezequiel Zamora-Ledezma [2], Michael Macías Pro [2], Joseph Guamán [1], Alexis Debut [1], Frank Alexis [3], Frederico B. De Sousa [4] and Christian Narváez-Muñoz [5,*]

[1] Universidad de las Fuerzas Armadas—ESPE, Sangolquí 171103, Ecuador; mggranda2@espe.edu.ec (M.G.); jaguaman19@espe.edu.ec (J.G.); apdebut@espe.edu.ec (A.D.)
[2] Laboratorio de Agroecosistemas y Cambio Climático—FAGROCLIM, Departamento de Ciencias Agrícolas, Facultad de Ingeniería Agrícola, Universidad Técnica de Manabí—UTM, Lodana 13132, Ecuador; ezequiel.zamora@utm.edu.ec (E.Z.-L.); michael.macias@utm.edu.ec (M.M.P.)
[3] Departamento de Ingeniería Química, Colegio de Ciencias e Ingeniería, Instituto de Energía y Materiales, Instituto de Microbiología, Universidad San Francisco de Quito (USFQ), Quito 170901, Ecuador; falexis@usfq.edu.ec
[4] Laboratório de Sistemas Poliméricos e Supramoleculares (LSPS)—Instituto de Física e Química, Universidade Federal de Itajubá (UNIFEI), Itajubá, MG 37500-903, Brazil; fredbsousa@unifei.edu.br
[5] Departamento de Ciencias de la Energía y Mecánica, Universidad de las Fuerzas Armadas—ESPE, Sangolquí 171103, Ecuador
* Correspondence: cpnarvaez1@espe.edu.ec

Highlights

What are the main findings?

- Multilayer electrospun nanofibrous membranes based on polyacrylonitrile (PAN), chitosan (CS), and Nylon 6 (N6) were engineered and mechanically optimized for the adsorption of hexavalent chromium and cadmium from water.
- The optimized CS–N6–PAN architecture achieved removal efficiencies above 80% for Cr^{6+} and approximately 79% for Cd^{2+} in synthetic solutions, while maintaining high performance in real river water.

What are the implications of these findings?

- These multilayer electrospun membranes, particularly with chitosan as the outer functional layer, offer a robust and environmentally friendly platform for heavy metal remediation in contaminated waters.
- The combination of high adsorption efficiency, mechanical stability, and effectiveness in real water matrices underscores their potential for scalable and sustainable water treatment applications.

Abstract

This study presents the fabrication and performance analysis of multilayer membranes produced by electrospinning using polyacrylonitrile (PAN), chitosan (CS), and Nylon 6 (N6) for the removal of chromium (Cr) and cadmium (Cd) from water. The electrospun membranes were configured in six different multilayer structures. The morphological and mechanical properties of the membranes were evaluated using SEM and tensile testing. Adsorption experiments were performed using synthetic and real water samples from the Cutuchi River. The multilayer membranes demonstrated metal ion removal efficiencies up to 80.81% for Cr^{6+} and 78.98% for Cd^{2+} in synthetic water, and similar performance in real samples. These results validate the use of multilayer electrospun membranes as an effective, environmentally friendly method for water purification applications.

check for updates

Academic Editor: Mataz Alcoutlabi

Received: 16 September 2025
Revised: 7 November 2025
Accepted: 26 November 2025
Published: 2 December 2025

Citation: Granda, M.; Zamora-Ledezma, E.; Macías Pro, M.; Guamán, J.; Debut, A.; Alexis, F.; De Sousa, F.B.; Narváez-Muñoz, C. Multilayer Electrospun Nanofibrous Membranes for Enhanced Heavy Metal Remediation. *Fibers* **2025**, *13*, 161. https://doi.org/10.3390/fib13120161

Copyright: © 2025 by the authors. Licensee MDPI, Basel, Switzerland. This article is an open access article distributed under the terms and conditions of the Creative Commons Attribution (CC BY) license (https://creativecommons.org/licenses/by/4.0/).

Keywords: membranes; nanofibers; heavy metals; adsorption; electrospinning

1. Introduction

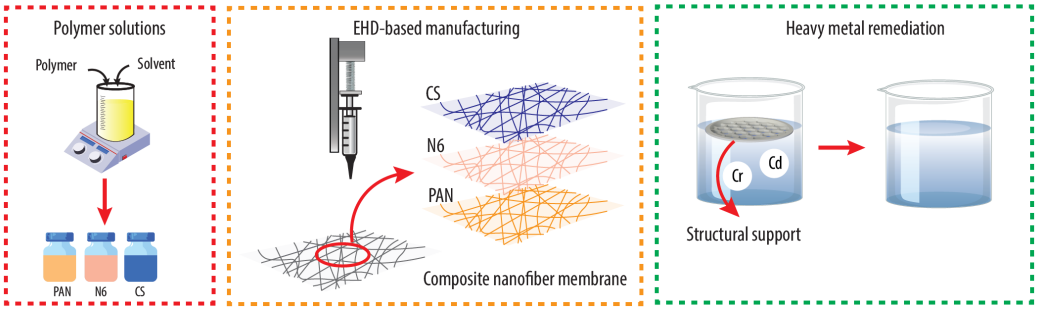
Water contamination by heavy metals constitutes a growing threat to human health and ecological balance due to their persistence, toxicity, and bioaccumulation [1,2]. Anthropogenic activities such as industrialization, mining, intensive agriculture, and uncontrolled urbanization have significantly increased the discharge of effluents contaminated with metals such as cadmium (Cd), lead (Pb), chromium (Cr), zinc (Zn), and nickel (Ni) into surface and groundwater bodies [3,4]. Since these contaminants are neither biodegradable nor transformable through natural processes, they pose a critical risk to living organisms, even at trace concentrations [5,6]. As a result, compliance with environmental regulations requires the implementation of efficient treatment technologies prior to the discharge or reuse of industrial wastewater.

Conventional treatment methods such as chemical precipitation, nanotechnology, ion exchange, and coagulation–flocculation have been widely employed for heavy metal removal [7]. However, these techniques present notable limitations, including high operational costs, low efficiency at trace concentrations, and the generation of large volumes of secondary sludge [8,9]. In recent years, alternative approaches such as adsorption, bioadsorption, and membrane-based separation have gained traction for their enhanced selectivity, operational simplicity, and potential for regeneration and reuse [10–12]. Among these emerging technologies, electrohydrodynamic (EHD)-based manufacturing—particularly electrospinning—has shown great promise in the development of nanostructured membranes for water purification [13,14]. Electrospinning enables the production of long, continuous nanofibers with high specific surface area, tunable porosity, and minimal environmental impact, all of which are advantageous for separation processes. The technique has seen rapid advancement and application in areas such as air and water filtration [15,16], catalysis [17,18], sensing [19,20], and energy storage [21,22].

In the context of heavy metal remediation, electrospun nanofibrous membranes (ENFMs) composed of functional polymers—such as polyacrylic acid (PAA), chitosan (CS), polyvinyl alcohol (PVA), polyethyleneimine (PEI), polypyrrole (PPy), polyacrylonitrile (PAN), polyaniline (PANI), and polyindoles (PIN)—have demonstrated high adsorption capacities for metal ions including Cu^{2+}, Pb^{2+}, Cd^{2+}, and Cr^{6+}. Despite their promising performance, a key limitation remains: many functional ENFMs exhibit poor mechanical stability in aqueous environments, limiting their practical use in dynamic or large-scale water treatment systems. To overcome this, recent efforts have focused on blending functional polymers with mechanically robust counterparts—such as PVA, PAN, and Nylon 6—to enhance structural integrity without sacrificing adsorption efficiency [23]. For instance, PAA/PVA hybrid ENFMs exhibit high removal efficiencies for heavy metals such as Cu^{2+}, Pb^{2+}, and Cd^{2+} [24,25]. Similarly, PEI/PVA ENFMs demonstrate effective adsorption capacities for Cu^{2+}, Cd^{2+}, and Pb^{2+} [26]. More advanced architectures, such as PAN/PANI–Nylon core–shell nanofiber membranes, functionalized with diethylenetriamine (DETA), have been developed to improve hydrophilicity, antifouling properties, and permeability, contributing to enhanced separation performance [27].

Among functional polymers, chitosan stands out as one of the most extensively studied materials due to its abundant $–NH_2$ (amine) and –OH (hydroxyl) groups [28]. These groups act as active binding sites, capable of forming coordination bonds, chelates, or electrostatic interactions (depending on the pH) with metal ions such as Pb^{2+}, Cd^{2+}, Cr^{3+}/Cr^{6+}, Cu^{2+}, Fe^{3+}, and Hg^{2+}. However, the production of defect-free, continuous CS-based electrospun

nanofibers presents significant challenges. These difficulties stem from chitosan's polyelectrolytic nature, limited solubility, and the poor spinnability of its solutions, which hinder the formation and collection of uniform nanofibers during the electrospinning process. A common strategy to address these issues involves blending chitosan with nonionic polymers such as polyvinyl alcohol or polyvinylpyrrolidone (PVP), which possess flexible molecular chains that facilitate fiber formation. While such blends can produce continuous nanofibers, the resulting materials often suffer from reduced mechanical integrity, limited uniformity, and poor collectability, thereby constraining their practical applicability. In this work, we proposed to introduce a gauze-based collector substrate, which enabled the formation of continuous, defect-free CS fibers. These fibers were subsequently integrated into a multilayer electrospun membrane composed of polyacrylonitrile, chitosan, and Nylon 6 (as shown in the Scheme 1). This hierarchical architecture, combined with a tailored fiber collection strategy, allows the membrane to harness the complementary properties of each polymer: PAN contributes antimicrobial activity [29], chitosan provides strong affinity toward heavy metal ions [30], and Nylon 6 imparts structural robustness and water stability [31]. The membranes were evaluated for their ability to passively adsorb heavy metals from water. Testing included both model aqueous solutions containing Cr^{6+} and Cd^{2+} ions as well as real-world samples taken from the Cutuchi River (Cotopaxi, Ecuador), which are known to contain heavy metals exceeding regulatory limits [32]. The study successfully demonstrated the membranes' effective heavy metal removal capacity, along with their high mechanical stability, confirming their significant potential for use in sustainable water treatment applications.



Scheme 1. Schematic representation of the electrospun nanofiber-based composite membrane. (**Left**) preparation of polymer solutions from PAN, N6, and CS. (**Center**) fabrication of a multilayer nanofibrous membrane by electrospinning. (**Right**) application of the composite membrane for the remediation of heavy metal ions in aqueous media.

2. Materials and Methods

2.1. Materials

The polymeric components used in this study were Nylon 6 (density 1.084 g/mL, Sigma-Aldrich, Quito, Ecuador), chitosan (90% deacetylated, Chemsavers, Miami, FL, USA), polyvinyl alcohol (PVA, 115 kDa, Loba Chemie, Quito, Ecuador), and polyacrylonitrile (PAN, 150 kDa, LookChem, Shanghai, China). The solvents employed were dimethylformamide (DMF, 99.5% purity, Fisher Scientific, Cali, Colombia), acetic acid (analytical grade, J.T. Baker), and formic acid (analytical grade, Fisher Scientific), chosen for their ability to fully dissolve the respective polymers and facilitate stable electrospinning. All materials were used as received without further purification, ensuring reproducibility and consistency in the preparation of electrospun nanofiber membranes.

2.2. Polymer Solution Preparation

Three polymer solutions were prepared for this study: Nylon 6, chitosan, and polyacrylonitrile. The N6 solution was prepared at a concentration of 22 wt% by dissolving 6.6 g of Nylon 6 in 23.4 g of formic acid (78%), yielding a total of 30 g of solution. The mixture was stirred using a magnetic stirrer at 125 rpm for 6 h at room temperature until a homogeneous and transparent solution was obtained. The CS solution was prepared in two steps. First, a 7 wt% polyvinyl alcohol solution was obtained by dissolving 2.1 g of PVA in 27.9 g of distilled water, followed by magnetic stirring at 125 rpm for 6 h. Then, a second solution was prepared by mixing the PVA solution with chitosan (3 wt%) in a 2:1 CS:PVA weight ratio. This mixture was stirred magnetically for 24 h until a homogeneous brownish polymer solution. For the PAN solution, 10 wt% PAN was dissolved in dimethylformamide to a total mass of 30 g. The components were weighed using an analytical balance and mixed in a beaker under magnetic stirring at 100 rpm for 8 h at room temperature, resulting in a uniform brown-colored solution.

2.3. Membrane Fabrication

Nanofiber fabrication was conducted using an EHD-TECH system equipped with a Genvolt, (Dublin, Ireland) 73030, 30 kV high-voltage source, a Cole Palmer (Vernon Hills, IL, USA) 788110C syringe pump, a spray head, and a steel collector plate. Polymer solutions were loaded into 10 mL NIPRO plastic syringes and injected through a 0.4 mm internal diameter stainless steel nozzle. The applied voltage (V) and flow rate (Q) were carefully adjusted to sustain a stable cone-jet mode, while other parameters—such as the polymer concentration—were maintained constant across multiple fabrication runs to ensure repeatability in membrane preparation. The morphology and size of the synthesized structures were investigated using a field emission gun scanning electron microscope (FEG-SEM, Mira3 Tescan). Samples were directly deposited onto aluminum stubs and imaged at accelerating voltages ranging from 3 to 5 kV.

2.4. Membrane Layer Distribution

To evaluate the efficiency of the multilayer membranes, six membrane models were designed by varying the order and arrangement of the three polymers investigated: PAN, CS, and N6. The layer configurations are depicted in Table 1.

Table 1. Multilayer membrane designs and polymer layer combinations.

Membrane	Components
M1	PAN/ CS/N6
M2	N6/CS/PAN
M3	N6/PAN/CS
M4	CS/PAN/N6
M5	CS/N6/PAN
M6	PAN/N6/CS

These variations allowed for a systematic study of how the polymer layer sequence influences the properties and performance of the multilayer membranes.

2.5. Metal Removal Tests

To evaluate the potential of the fabricated membranes for the removal of Cr^{6+} and Cd^{2+}, preliminary adsorption tests were conducted using: (a) synthetic reference samples (SRS) prepared in the laboratory and (b) raw residual water samples (RRS) collected from the Cutuchi River, located in Latacunga, Cotopaxi, Ecuador. All procedures related to

sample preparation, metal retention assays, and post-treatment metal quantification were performed at the Chemical and Biotechnological Analysis Laboratory of the Universidad Técnica de Manabí.

Synthetic reference samples (SRS): SRS were prepared following the methodology described by [33] using high-purity, ICP-OES-grade reagents, including chromium and cadmium standard solutions (1000 µg/mL and 1000 µg/L, respectively) and analytical-grade nitric acid. Ultrapure water (≥18.2 MΩ·cm at 25 °C) from a Barnstead EasyPure II system was used for all dilutions. Initial stock solutions of Cd^{2+} and Cr^{6+} were prepared at a concentration of 10 ppm each by appropriate dilution of the commercial standards in 2% (*v/v*) nitric acid to ensure metal ion stability and prevent precipitation or adsorption to container walls. Elemental concentrations were subsequently analyzed using an ICP-OES instrument (Perkin Elmer Optima 3000 XL). Subsequently, serial dilutions were prepared at concentrations of 5, 2, 1, 0.8, 0.5, 0.25, and 0.05 µg/mL to construct calibration curves for ICP-OES quantification. These dilutions were used to evaluate the analytical performance of the method in terms of linearity (R^2), limit of quantification (LOQ), and limit of detection (LOD), as detailed in Supplementary Materials. Working reference solutions for adsorption experiments were then prepared with final concentrations of 2.3 mg/L for Cd^{2+} and 1.6 mg/L for Cr^{6+}, corresponding to typical contamination levels found in industrial effluents and environmental water bodies.

Real water sample collection and preparation (RRS): RRS were collected from the Cutuchi River using pre-cleaned, acid-washed high-density polyethylene (HDPE) bottles following standard sampling protocols. Sampling was performed at midstream locations, approximately 20–30 cm below the water surface, to obtain representative samples. Immediately after collection, the samples were acidified to pH < 2 with concentrated nitric acid (0.5% *v/v* final concentration) to prevent metal precipitation and microbial degradation, and subsequently stored at 4 °C during transport to preserve their physicochemical integrity. Upon arrival at the laboratory, samples were equilibrated to room temperature (approximately 25 °C) and filtered under vacuum through Whatman 42 filter paper (pore size 2.5 µm) to remove suspended solids and particulate matter, ensuring compatibility with both membrane testing and analytical instrumentation. The filtered samples were then divided into aliquots for specific analyses. Preliminary measurements included pH determination using a calibrated pH meter, electrical conductivity assessment using a conductivity probe, and baseline metal content analysis via ICP-OES to quantify the initial concentrations of target contaminants (Cd^{2+} and Cr^{6+}), along with potentially interfering ions such as Ca^{2+}, Mg^{2+}, Fe^{3+}, and Cu^{2+}. Following this complete characterization, all aliquots were stored at 4 °C until the subsequent adsorption experiments.

Membrane adsorption experimental protocol: Membrane specimens with dimensions of 4 cm × 4 cm were cut from the electrospun multilayer membranes using stainless steel scissors and weighed prior to each experiment to ensure consistency. Each membrane sample was then immersed in a glass beaker containing 50 mL of either SRS or RRS solution at room temperature (25 ± 2 °C). To ensure uniform contact between the membrane surface and the metal-containing solution while preventing structural fiber collapse, a custom-designed support frame was employed. The beakers were placed on an orbital shaker and agitated continuously at 50 rpm for 1 h. This agitation speed was selected to ensure sufficient mixing and mass transfer without inducing mechanical stress that could damage the fibrous structure or cause fiber detachment. After the contact period, the membranes were carefully removed using clean forceps, briefly rinsed with ultrapure water to remove loosely bound contaminants, and set aside for further analysis. The treated solutions were collected, filtered through 0.45 µm syringe filters to eliminate any detached fibers or particulates, and acidified with 2% (*v/v*) nitric acid for preservation prior to analysis.

The final metal ion concentrations in both SRS and RRS samples were quantified using inductively coupled plasma optical emission spectrometry (ICP-OES), with the model and operating parameters detailed in Supplementary Materials. Metal removal efficiency (%) was determined according to Equation (1):

$$\text{Removal Efficiency (\%)} = \frac{C_0 - C_f}{C_0} \times 100 \quad (1)$$

where C_0 represents the initial metal ion concentration (mg/L) and C_f denotes the final concentration (mg/L) after membrane treatment. All experiments were performed in triplicate to ensure reproducibility, and mean values with standard deviations are reported in Section 3.4.

3. Results and Discussion

3.1. Preliminary Electrospinning Trials

Prior to the fabrication of multilayered membranes, systematic electrospinning trials were carried out using chitosan, polyacrylonitrile, and Nylon 6 to establish optimal processing conditions. These trials aimed to identify critical parameters for stable jet formation and consistent film deposition. Key observations include

- Chitosan in acetic acid: When dissolved in 70% acetic acid at 2–3 wt%, CS generally failed to produce continuous fibers, resulting instead in either no structures or beaded fibers (see Figure 1a,b). Increasing the acetic acid concentration to 90% enabled the formation of stable fibers with fewer bead defects at 3 wt% CS, as shown in Figure 1c. In comparison, PVA in water typically required higher concentrations (around 7 wt%) together with optimized electrospinning parameters to produce uniform membranes; otherwise, the resulting structures were weak or of poor quality.
- PAN in DMF: As demonstrated in our previous research [34,35], fiber quality improved with increasing concentration. Low concentrations (5 wt%) failed to form membranes, while 12 wt% at lower voltages (10 kV) produced uniform, defect-free fibers, indicating that higher polymer content enhances stability and film integrity.
- Nylon 6 in formic acid: Continuous membranes were obtained only at high concentrations (≥18 wt%) and low flow rates (10 µL/h) with moderate voltages (14–16 kV). Lower concentrations resulted in beaded fibers, highlighting the importance of sufficient viscosity and solution conductivity for stable film formation [36].

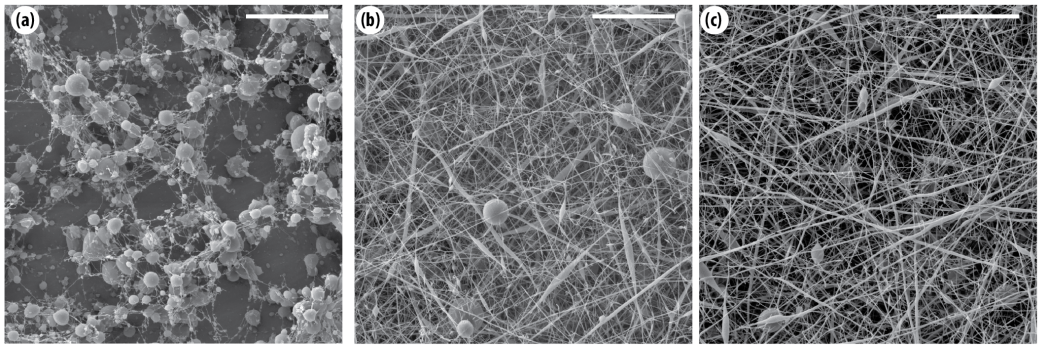


Figure 1. SEM images showing the morphology of structures obtained from chitosan solutions prepared in: (**a**) 70% acetic acid at 2 wt% CS, (**b**) 70% acetic acid at 3 wt% CS, and (**c**) 90% acetic acid at 3 wt% CS. Scale bars represent 5 µm.

3.2. Fiber Morphology

The morphology of electrospun fibers—polyacrylonitrile, chitosan, and Nylon 6—was characterized using SEM imaging. Fiber diameter distributions were statistically analyzed

with ImageJ 1.54 software, based on measurements of 82 individual fibers. Each polymer solution was prepared at the optimized concentrations described in the previous section. Initial attempts to fabricate ENFMs from a 2 wt% CS solution using a conventional aluminum foil collector produced bead-rich fibers that were mechanically fragile and strongly adhered to the substrate (Figure 2left). To address these limitations, membranes were subsequently collected on a gauze substrate, whose porous and textured surface improved fiber anchoring and reduced charge accumulation, thereby enhancing fiber morphology and facilitating detachment (Figure 2right). The multiple anchoring points provided by the gauze suppressed bead formation and promoted fiber release, yielding more continuous and mechanically robust fiber networks (Figure 3a). CS fibers displayed a strong dependence on the collection substrate. Fibers deposited on aluminum foil exhibited a smaller mean diameter (0.12 ± 0.31 µm) compared to those collected on gauze (0.31 ± 0.06 µm) (Figure 3e). This variation is attributed to substrate-induced effects, where differences in surface interactions and electrostatic grounding influence jet elongation, solvent evaporation, and fiber deposition dynamics. The optimized electrospinning parameters for CS were: flow rate (Q) = 0.5 mL/h, applied voltages of +15 kV and −1 kV, and a collector distance (d) of 14 cm.

In contrast to CS, both PAN and N6 exhibited far greater process stability during electrospinning. SEM analysis confirmed that PAN fibers formed a uniform, bead-free morphology under the following conditions: Q = 1 mL/h, applied voltages of +10 kV and −12 kV, and a collector distance of 14 cm (Figure 3b). This stability can be attributed to the good solubility and high chain flexibility of PAN, which facilitate stable jet formation and continuous fiber deposition [34]. PAN fibers had an average diameter of 0.245 ± 0.07 µm, consistent with previous reports under comparable solution properties and electrospinning conditions. N6 also produced highly uniform, bead-free fibers at a flow rate of 10 µL/h, applied voltages of +15 s kV and −11 kV, and a collector distance of 19 cm (Figure 3c). Unlike CS, the N6 solution exhibited enhanced jet stability throughout the process, reflecting a favorable balance between viscosity, conductivity, and surface tension that supports the formation of defect-free fibers. N6 fibers displayed the smallest diameter among the studied polymers, averaging 0.14 ± 0.03 µm. The reduced diameter of N6 fibers is attributed to the relatively higher conductivity and dielectric constant of the solution, which intensify electrostatic stretching forces on the polymer jet and promote further thinning prior to solidification.

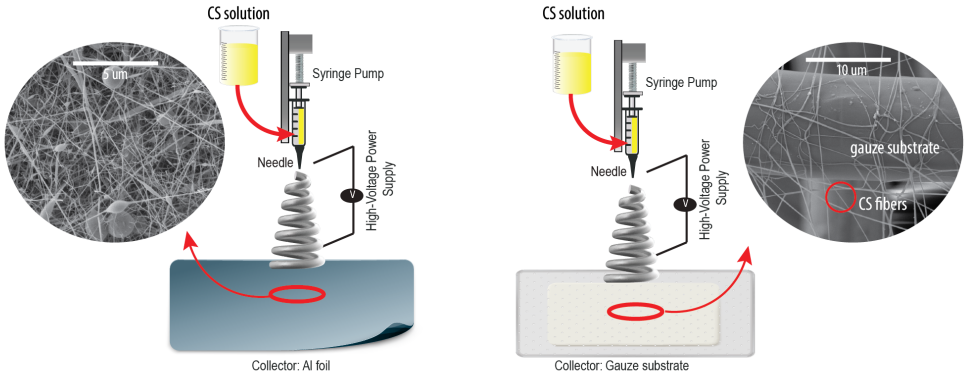


Figure 2. SEM images showing the morphology of chitosan fibers collected on (**left**) aluminum foil and (**right**) gauze substrate.

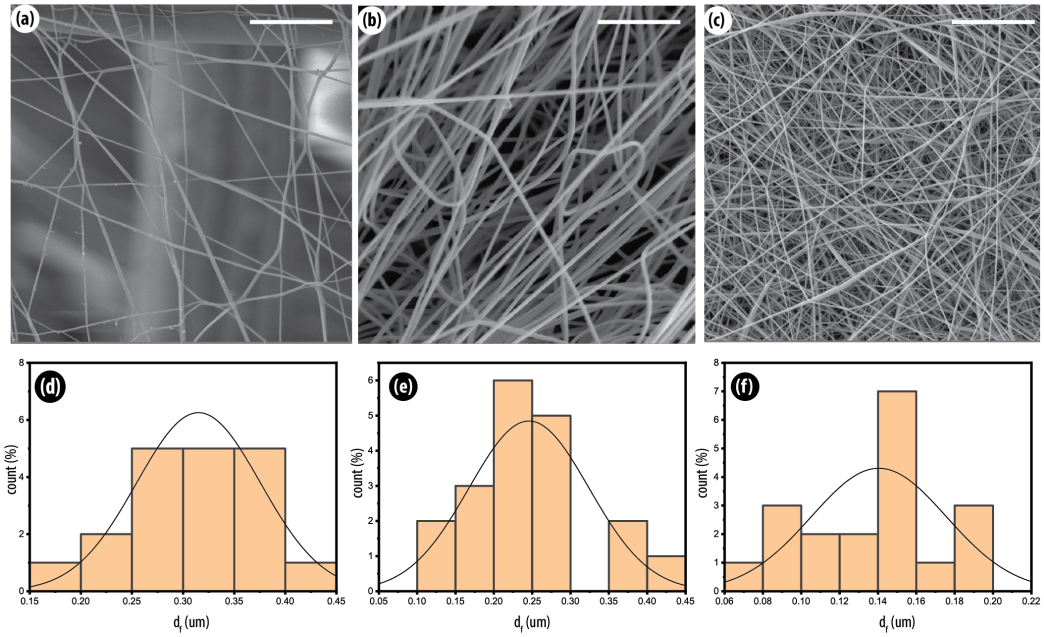


Figure 3. SEM micrographs of electrospun membranes fabricated from (**a**) CS, (**b**) PAN, and (**c**) N6, highlighting differences in fiber morphology. Scale bars correspond to 5 µm for CS and N6, and 4.5 µm for PAN. The corresponding fiber diameter distributions are shown in (**d**) CS, (**e**) PAN, and (**f**) N6.

3.3. Mechanical Properties

The mechanical behavior of electrospun membranes was evaluated through uniaxial tensile tests on both single-material specimens—composed of chitosan, polyacrylonitrile, and Nylon 6—and multilayer membranes formed from various combinations of these materials, in order to determine their suitability for filtration applications, which require a balance of mechanical strength and flexibility under load. As shown in Figure 4a, the single-material membranes exhibited distinct mechanical profiles: CS showed brittle behavior with a maximum elongation of approximately 6%, while N6 and PAN demonstrated more ductile responses, with elongations reaching up to 30% and over 40%, respectively. The yield strengths followed a similar trend, with CS: 0.12 ± 0.019 MPa, PAN: 1.89 ± 0.039 MPa, and N6: 2.10 ± 0.024 MPa, confirming that PAN and N6 are significantly stronger and more stretchable than CS and thus more appropriate for structural applications. These differences arise from both the intrinsic molecular characteristics of the polymers and the unique microstructure of electrospun mats. Unlike bulk materials, electrospun membranes are composed of porous, nanostructured, and randomly oriented fiber networks, where mechanical behavior depends on fiber alignment, bonding, and inter-fiber friction. At the molecular level, chitosan contains hydroxyl and amino groups that form strong intramolecular hydrogen bonds, leading to a rigid structure with limited chain mobility and low elongation. In contrast, PAN possesses polar nitrile groups that promote dipole–dipole interactions, resulting in high tensile strength and moderate flexibility. N6, on the other hand, contains amide groups capable of forming intermolecular hydrogen bonds and exhibits a semicrystalline morphology, which together confer high strength and toughness.

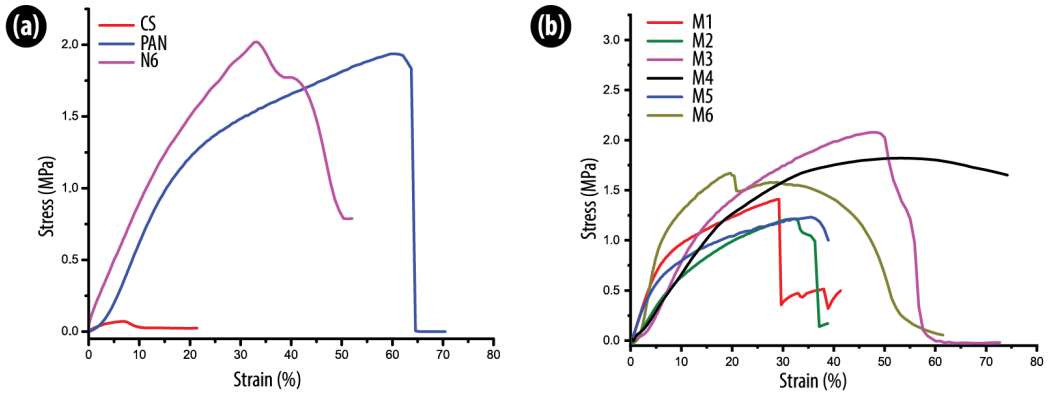


Figure 4. Mechanical properties of electrospun membranes evaluated through uniaxial tensile tests. (**a**) Single-material membranes (CS, PAN, and N6). (**b**) Multilayer membranes composed of various polymer combinations, highlighting the influence of layer arrangement on tensile strength and elongation.

Building on these results, multilayer membranes were fabricated using six different layer configurations, all produced under identical electrospinning conditions, using the same polymer batches and equal collection times. The mechanical properties of these multilayer systems, presented in Figure 4b, showed maximum tensile strengths ranging from 1.23 MPa to 2.10 MPa, and elongations between 18% and 48%. Notably, the PAN/N6/CS combination yielded the highest performance in both strength (2.10 ± 0.014 MPa) and elongation (48%), while the N6/PAN/CS stack exhibited the lowest strength (1.23 ± 0.011 MPa) and the CS/N6/PAN structure showed the lowest strain (18%). These differences are primarily attributed to interfacial phenomena occurring between adjacent layers. As shown in Figure 5, a partial separation between layers in the M6 membrane can be linked to variations in solvent composition, polymer chain mobility, and surface charge density among the chitosan, Nylon 6, and polyacrylonitrile layers, all of which influence fiber deposition and interfacial adhesion. The formation of hydrogen bonds between hydroxyl groups in CS and amide groups in N6 promotes local adhesion; however, incomplete wetting or differential solvent evaporation may lead to regions of weak bonding. Furthermore, electrostatic repulsion arising from residual surface charges on sequentially deposited fibers may hinder full interpenetration across interfaces [37]. Collectively, these effects result in the slight interfacial separation observed in the cross-sectional SEM micrograph, highlighting the delicate balance between cohesive and adhesive forces within multilayer electrospun assemblies.

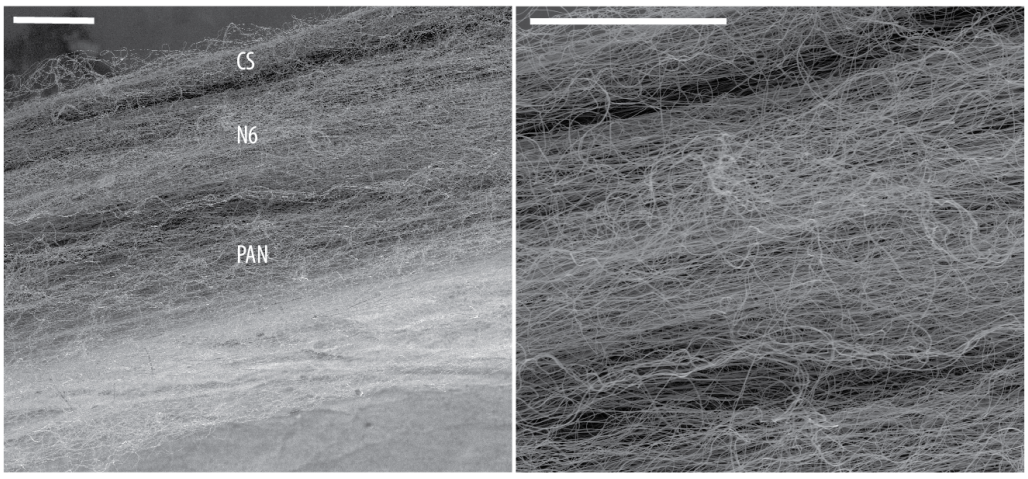


Figure 5. SEM micrographs illustrating the multilayer structure of the M6 membrane, showing its three distinct layers. Scale bars represent 100 µm.

3.4. Adsorption Performance of Electrospun Membranes

Heavy Metal Removal in Synthetic Water Samples: The efficacy of electrospun multilayer membranes for Cr^{6+} and Cd^{2+} adsorption was rigorously investigated using synthetic aqueous solutions. Standard solutions were prepared at a concentration of 2.3 mg/L for Cd^{2+} and 1.6 mg/L for Cr^{6+}. Square membranes were immersed in the prepared solutions and subjected to continuous agitation at 50 rpm for 1 h to promote homogeneous mass transfer while minimizing excessive shear stress. Table 2 presents the percentage removal observed across three experimental trials, highlighting variations in membrane configuration and performance. In Trial 1, removal efficiencies were generally low due to membrane deformation and fiber collapse during agitation. This structural integrity was significantly compromised, reducing the accessible surface area for adsorption, thereby affecting adsorption performance. To address this drawback, a structural support was incorporated following the approach reported in [35]. Trials 2 and 3 implemented this modification, ensuring the preservation of laminar morphology and maintaining the cross-sectional integrity of the fibrous mats throughout the experiments. Among the six evaluated membrane configurations, M6 (CS/N6/PAN) consistently demonstrated superior removal performance across both metal ions, achieving nearly 80% removal for cadmium ion and over 80% for chromium ion in Trials 2 and 3. This enhanced efficacy is hypothesized to stem from the strategic placement of the CS layer as the outermost functional surface. This outermost placement ensures an abundant density of readily accessible functional groups, providing optimal binding sites conducive to effective metal ion chelation and adsorption.

Heavy Metal Removal from Cutuchi River Water: Following the comprehensive evaluation of all six electrospun membranes using synthetic water enriched with Cd and Cr, the two configurations exhibiting the most promising removal efficiencies—membranes M5 (CS/PAN/N6) and M6 (CS/N6/PAN)—were selected for further validation using actual water samples collected from the Cutuchi River, located in Latacunga, Ecuador. This step is critical for assessing the practical applicability and robustness of the membranes in a more complex and representative environmental matrix.

Table 2. Percentage removal of Cd^{2+} and Cr^{6+} from synthetic water using electrospun membranes.

Membrane	Cd^{2+} Removal (%)			Cr^{6+} Removal (%)		
	Trial 1	Trial 2	Trial 3	Trial 1	Trial 2	Trial 3
M1 (N6/CS/PAN)	0.00	64.20	61.15	0.00	45.13	55.23
M2 (N6/PAN/CS)	0.00	71.43	71.43	0.00	57.67	67.57
M3 (PAN/N6/CS)	0.00	71.55	71.55	0.00	46.89	49.81
M4 (PAN/CS/N6)	0.00	74.22	74.22	0.00	60.07	65.17
M5 (CS/PAN/N6)	0.00	75.33	75.43	0.00	56.89	65.93
M6 (CS/N6/PAN)	5.06	77.64	78.98	3.65	75.72	80.81

The results, summarized in Table 3, indicate that both membranes exhibited high removal efficiencies for both Cd^{2+} and Cr^{6+} in the Cutuchi River water samples. Notably, membrane M6 (CS-N6-PAN) achieved up to 77.1% removal of Cd and 82.8% of Cr, confirming its superior adsorption capacity even in the presence of competing ions and organic matter characteristic of natural waters. This enhanced performance is primarily attributed to the intrinsic functional properties of the quaternized starch layer. The CS polymer provides a high density of free electron pairs on its amino ($–NH_2$) and hydroxyl (–OH) groups. These functional groups are critical for enabling effective ion-exchange interactions and robust chelation with diverse metal ions, likely involving coordination of the metal ions with oxygen atoms from the hydroxyl groups [38,39]. The surface chemistry of CS thus plays a critical and multifaceted role in the adsorption mechanism, contributing to

the high affinity toward heavy metals such as Cd and Cr under the tested conditions, even within the complex matrix of natural river water. Future studies could involve long-term continuous flow experiments and regeneration studies to fully assess the economic viability and sustainability of these advanced adsorptive membranes.

Table 3. Heavy metal removal from Cutuchi River water using selected electrospun membranes.

Membrane	Cd^{2+} (mg/L)	Cr^{6+} (mg/L)	Cd^{2+} Removal (%)	Cr^{6+} Removal (%)
M5	2.330	1.570	74.3	75.2
M6	2.251	1.551	77.1	82.8

4. Conclusions

Electrospun membranes were successfully fabricated using polymer solutions of PAN, CS, and N6 at various concentrations. The optimal concentrations for producing homogeneous fibers were determined to be 12 wt% for PAN, 2 wt% for CS, and 22 wt% for N6. The CS membranes exhibited an average fiber diameter of $d_f = 0.12 \pm 0.306$ µm and a mechanical strength of 0.12 MPa. In comparison, PAN and N6 fibers had average diameters of 0.245 ± 0.07 µm and 0.14 ± 0.03 µm, with corresponding mechanical strengths of 1.89 MPa and 2.1 MPa, respectively. The incorporation of PAN and N6 notably enhanced the structural stability and mechanical performance of the multilayer membranes.

The adsorption capacity of the membranes was assessed using both synthetic water samples containing 2 mg/L of chromium and cadmium, and natural river water samples from the Cutuchi River, which included organic contaminants. All six multilayer configurations demonstrated high removal efficiencies in synthetic tests, reaching up to 78.98% for Cd^{2+} and 80.81% for Cr^{6+}. Based on these results, membranes M5 (CS/PAN/N6) and M6 (CS/N6/PAN) were selected for further evaluation with natural water samples. Among them, membrane M6 exhibited superior adsorption performance, achieving removal efficiencies of up to 77% for Cd^{2+} and 82.8% for Cr^{6+}.

Supplementary Materials: The following supporting information can be downloaded at https://www.mdpi.com/article/10.3390/fib13120161/, Figure S1: Calibration curves for cadmium (Cd) and chromium (Cr) obtained using ICP-OES.

Author Contributions: Conceptualization, E.Z.-L. and C.N.-M.; methodology, C.N.-M., J.G. and M.G.; software, M.G. and J.G.; validation, E.Z.-L. and M.M.P.; formal analysis, C.N.-M., E.Z.-L., F.A. and F.B.D.S.; investigation, M.G. and C.N.-M.; resources, F.B.D.S. and C.N.-M.; data curation, M.G., C.N.-M., E.Z.-L., M.M.P., F.A. and F.B.D.S.; writing—original draft, M.G. and C.N.-M.; writing—review & editing, C.N.-M., F.A., and F.B.D.S.; visualization, A.D. and J.G.; supervision, C.N.-M. All authors have read and agreed to the published version of the manuscript.

Funding: This research was funded by Conselho Nacional de Desenvolvimento Científico e Tecnológico (CNPq) grant number 303311/2024-0 and Fundação de Amparo à Pesquisa do Estado de Minas Gerais (FAPEMIG), grant numbers APQ-04537-22, RED-00045-23, and APQ-00144-24.

Data Availability Statement: The original contributions presented in this study are included in the article. Further inquiries can be directed to the corresponding author.

Acknowledgments: The authors would like to express their sincere appreciation to Joan Manuel Rodríguez-Díaz for his technical support, and insightful discussions throughout the course of this research. Rodríguez-Díaz is affiliated with the Laboratory of Chemical Analysis and Biotechnology at the Research Institute of the Universidad Técnica de Manabí, and the Department of Chemical Processes, Biotechnology, and Food of the Faculty of Engineering and Applied Sciences. In addition, authors would like to thank Conselho Nacional de Desenvolvimento Científico e Tecnológico

(CNPq) grant number 303311/2024-0 and Fundação de Amparo à Pesquisa do Estado de Minas Gerais (FAPEMIG), grant numbers APQ-04537-22, RED-00045-23, and APQ-00144-24.

Conflicts of Interest: The authors declare that they have no conflicts of interest.

References

1. Kaur, R.; Sharma, S.; Kaur, H. Heavy metals toxicity and the environment. *J. Pharmacogn. Phytochem.* **2019**, *1*, 247–249.
2. Zamora-Ledezma, C.; Negrete-Bolagay, D.; Figueroa, F.; Zamora-Ledezma, E.; Ni, M.; Alexis, F.; Guerrero, V.H. Heavy metal water pollution: A fresh look about hazards, novel and conventional remediation methods. *Environ. Technol. Innov.* **2021**, *22*, 101504. [CrossRef]
3. Ali, H.; Khan, E.; Ilahi, I. Environmental chemistry and ecotoxicology of hazardous heavy metals: Environmental persistence, toxicity, and bioaccumulation. *J. Chem.* **2019**, *2019*, 6730305. [CrossRef]
4. Mendonça, N.E.; Leão, C.A.; Alexis, F.; Ochoa-Herrera, V.; Zambrano-Romero, A.; Nobuyasu, R.S., Jr.; Miguez, F.B.; De Sousa, F.B. Exploiting Spiropyran Solvatochromism for Heavy Metal Ion Detection in Aqueous Solutions. *ACS Omega* **2025**, *10*, 36412–36420. [CrossRef] [PubMed]
5. Rice, E.W.; Baird, R.B.; Eaton, A.D.; Clesceri, L.S. *Standard Methods for the Examination of Water and Wastewater*; American Public Health Association, American Water Works Association and Water Environment Federation: Washington, DC, USA, 2012.
6. Rehman, K.; Fatima, F.; Waheed, I.; Akash, M.S.H. Prevalence of exposure of heavy metals and their impact on health consequences. *J. Cell. Biochem.* **2018**, *119*, 157–184. [CrossRef] [PubMed]
7. Guerra, F.D.; Attia, M.F.; Whitehead, D.C.; Alexis, F. Nanotechnology for environmental remediation: Materials and applications. *Molecules* **2018**, *23*, 1760. [CrossRef] [PubMed]
8. Fu, F.; Wang, Q. Removal of heavy metal ions from wastewaters: A review. *J. Environ. Manag.* **2011**, *92*, 407–418. [CrossRef]
9. Crini, G.; Lichtfouse, E. Advantages and disadvantages of techniques used for wastewater treatment. *Environ. Chem. Lett.* **2019**, *17*, 145–155. [CrossRef]
10. Shrestha, R.; Ban, S.; Devkota, S.; Sharma, S.; Joshi, R.; Tiwari, A.P.; Kim, H.Y.; Joshi, M.K. Technological trends in heavy metals removal from industrial wastewater: A review. *J. Environ. Chem. Eng.* **2021**, *9*, 105688. [CrossRef]
11. Guizard, C.; Bac, A.; Barboiu, M.; Hovnanian, N. Hybrid organic-inorganic membranes with specific transport properties: Applications in separation and sensors technologies. *Sep. Purif. Technol.* **2001**, *25*, 167–180. [CrossRef]
12. Wang, W.; Hao, X.; Yan, Y.; Sun, R.; Petit, E.; Moderne, M.; Li, J.; Liu, J.; Wu, H.; Qi, K.; et al. 2D vermiculite nanolaminated membranes for efficient organic solvent nanofiltration. *Adv. Funct. Mater.* **2025**, *35*, 2410635. [CrossRef]
13. Mohamad, S.H.; Idris, M.I.; Abdullah, H.Z.; Ismail, A.F. Short review of ultrafiltration of polymer membrane as a self-cleaning and antifouling in the wastewater system. *Adv. Mater. Res.* **2013**, *795*, 318–323. [CrossRef]
14. Narváez-Muñoz, C.; Zamora-Ledezma, C.; Carrión-Matamoros, L.M.; Guerrero, I.E.; Debut, A.; Vizuete, K.; Haro, E.E.; López López, A.; Zamora-Ledezma, E. Influence of ultrasonication on the properties of hybrid electrospun polyacrylonitrile and silver nanoparticles fibers and their potential use in water decontamination. In *Applied Technologies, Proceedings of the Third International Conference, ICAT 2021, Quito, Ecuador, 27–29 October 2021*; Springer: Berlin/Heidelberg, Germany; pp. 176–188.
15. Wu, S.; Li, K.; Shi, W.; Cai, J. Preparation and performance evaluation of chitosan/polyvinylpyrrolidone/polyvinyl alcohol electrospun nanofiber membrane for heavy metal ions and organic pollutants removal. *Int. J. Biol. Macromol.* **2022**, *210*, 76–84. [CrossRef] [PubMed]
16. Zhang, L.; Li, L.; Wang, L.; Nie, J.; Ma, G. Multilayer electrospun nanofibrous membranes with antibacterial property for air filtration. *Appl. Surf. Sci.* **2020**, *515*, 145962. [CrossRef]
17. Borban, B.; Gohain, M.B.; Yadav, D.; Karki, S.; Ingole, P.G. Nano-electrospun membranes: Green solutions for diverse industrial needs. *J. Hazard. Mater. Adv.* **2023**, *12*, 100373. [CrossRef]
18. Netto, J.F.Z.; Miguez, F.B.; Bahia, S.B.; Bolais-Ramos, L.G.; Verano-Braga, T.; Trigueiro, J.P.; Nobuyasu, R.S.; Brandao, T.A.; De Sousa, F.B. Core-sheath organic-inorganic hybrid electrospun fibers for organophosphorus heterogeneous catalysis. *J. Environ. Chem. Eng.* **2024**, *12*, 113267. [CrossRef]
19. Wu, L.; Song, Y.; Xing, S.; Li, Y.; Xu, H.; Yang, Q.; Li, Y. Advances in electrospun nanofibrous membrane sensors for ion detection. *RSC Adv.* **2022**, *12*, 34866–34891. [CrossRef]
20. Miguez, F.B.; Trigueiro, J.P.; Lula, I.; Moraes, E.S.; Atvars, T.D.; de Oliveira, L.F.; Alexis, F.; Nobuyasu, R.S.; De Sousa, F.B. Photochromic sensing of La^{3+} and Lu^{3+} ions using poly (caprolactone) fibers doped with spiropyran dyes. *J. Photochem. Photobiol. A Chem.* **2024**, *452*, 115568. [CrossRef]
21. Liu, X.; Zhang, Y.; Guo, X.; Pang, H. Electrospun metal–organic framework nanofiber membranes for energy storage and environmental protection. *Adv. Fiber Mater.* **2022**, *4*, 1463–1485. [CrossRef]

22. Sudário, A.C.; dos Santos, L.P.; Morais, D.C.; Tonon, G.J.; Ferreira, I.D.; Moreira, R.P.; Alves, J.d.F.; de Oliveira, L.F.; dos Santos Junior, G.A.; de Sousa, F.B.; et al. Electrospun PAN-derived carbon nanofibers enabling superior supercapacitor performance with Quinone redox electrolytes. *J. Electroanal. Chem.* **2025**, *996*, 119356. [CrossRef]
23. Zhu, F.; Zheng, Y.M.; Zhang, B.G.; Dai, Y.R. A critical review on the electrospun nanofibrous membranes for the adsorption of heavy metals in water treatment. *J. Hazard. Mater.* **2021**, *401*, 123608. [CrossRef]
24. Xiao, S.; Shen, M.; Ma, H.; Guo, R.; Zhu, M.; Wang, S.; Shi, X. Fabrication of water-stable electrospun polyacrylic acid-based nanofibrous mats for removal of copper (II) ions in aqueous solution. *J. Appl. Polym. Sci.* **2010**, *116*, 2409–2417. [CrossRef]
25. Zhang, S.; Shi, Q.; Christodoulatos, C.; Meng, X. Lead and cadmium adsorption by electrospun PVA/PAA nanofibers: Batch, spectroscopic, and modeling study. *Chemosphere* **2019**, *233*, 405–413. [CrossRef] [PubMed]
26. Min, M.; Shen, L.; Hong, G.; Zhu, M.; Zhang, Y.; Wang, X.; Chen, Y.; Hsiao, B.S. Micro-nano structure poly (ether sulfones)/poly (ethyleneimine) nanofibrous affinity membranes for adsorption of anionic dyes and heavy metal ions in aqueous solution. *Chem. Eng. J.* **2012**, *197*, 88–100. [CrossRef]
27. Almasian, A.; Giahi, M.; Fard, G.C.; Dehdast, S.; Maleknia, L. Removal of heavy metal ions by modified PAN/PANI-nylon core-shell nanofibers membrane: Filtration performance, antifouling and regeneration behavior. *Chem. Eng. J.* **2018**, *351*, 1166–1178. [CrossRef]
28. Rinaudo, M. Chitin and chitosan: Properties and applications. *Prog. Polym. Sci.* **2006**, *31*, 603–632. [CrossRef]
29. Zhang, L.; Aboagye, A.; Kelkar, A.; Lai, C.; Fong, H. A review: Carbon nanofibers from electrospun polyacrylonitrile and their applications. *J. Mater. Sci.* **2014**, *49*, 463–480. [CrossRef]
30. Mallik, A.K.; Kabir, S.F.; Rahman, F.B.A.; Sakib, M.N.; Efty, S.S.; Rahman, M.M. Cu (II) removal from wastewater using chitosan-based adsorbents: A review. *J. Environ. Chem. Eng.* **2022**, *10*, 108048. [CrossRef]
31. Abd Halim, N.S.; Wirzal, M.D.H.; Bilad, M.R.; Md Nordin, N.A.H.; Adi Putra, Z.; Mohd Yusoff, A.R.; Narkkun, T.; Faungnawakij, K. Electrospun nylon 6, 6/ZIF-8 nanofiber membrane for produced water filtration. *Water* **2019**, *11*, 2111. [CrossRef]
32. Guevara, M.A.R.; Cepeda, Y.V.M.; Jiménez, B.D.C.; Sangucho, B.J.C.; Lugmaña, A.Y.J. El río Cutuchi, contaminante que fluye en nuestra sociedad y la afecta. *RECIMUNDO* **2024**, *8*, 51–60. [CrossRef]
33. Esfahani, A.R.; Zhang, Z.; Sip, Y.Y.L.; Zhai, L.; Sadmani, A.A. Removal of heavy metals from water using electrospun polyelectrolyte complex fiber mats. *J. Water Process Eng.* **2020**, *37*, 101438. [CrossRef]
34. Narváez-Muñoz, C.; Zamora-Ledezma, C.; Ryzhakov, P.; Pons-Prats, J.; Elango, J.; Mena, C.; Navarrete, F.; Morales-Flórez, V.; Cano-Crespo, R.; Segura, L.J. Improving glass-fiber epoxy composites via interlayer toughening with polyacrylonitrile/multiwalled carbon nanotubes electrospun fibers. *J. Appl. Polym. Sci.* **2023**, *140*, e53400. [CrossRef]
35. Narváez-Muñoz, C.; Ponce, S.; Durán, C.; Aguayo, C.; Portero, C.; Guamán, J.; Debut, A.; Granda, M.; Alexis, F.; Zamora-Ledezma, E.; et al. Polyacrylonitrile/Silver Nanoparticles Composite for Catalytic Dye Reduction and Real-Time Monitoring. *Polymers* **2025**, *17*, 1762. [CrossRef] [PubMed]
36. Pant, H.R.; Bajgai, M.P.; Yi, C.; Nirmala, R.; Nam, K.T.; Baek, W.i.; Kim, H.Y. Effect of successive electrospinning and the strength of hydrogen bond on the morphology of electrospun nylon-6 nanofibers. *Colloids Surfaces A Physicochem. Eng. Asp.* **2010**, *370*, 87–94. [CrossRef]
37. Eda, G.; Shivkumar, S. Bead-to-fiber transition in electrospun polystyrene. *J. Appl. Polym. Sci.* **2007**, *106*, 475–487. [CrossRef]
38. Vold, I.M.; Vårum, K.M.; Guibal, E.; Smidsrød, O. Binding of ions to chitosan—Selectivity studies. *Carbohydr. Polym.* **2003**, *54*, 471–477. [CrossRef]
39. Caicho-Caranqui, J.; Vivanco, G.; Egas, D.A.; Chuya-Sumba, C.; Guerrero, V.H.; Ramirez-Cando, L.; Reinoso, C.; De Sousa, F.B.; Leon, M.; Ochoa-Herrera, V.; et al. Non-modified cellulose fibers for toxic heavy metal adsorption from water. *Adsorption* **2025**, *31*, 18. [CrossRef]

Disclaimer/Publisher's Note: The statements, opinions and data contained in all publications are solely those of the individual author(s) and contributor(s) and not of MDPI and/or the editor(s). MDPI and/or the editor(s) disclaim responsibility for any injury to people or property resulting from any ideas, methods, instructions or products referred to in the content.